

08
Study of the Effect of Growth Temperature on the Properties of Nitrogen-Doped Carbon Nanotubes for Designing Nanopiezotronic Devices

© M.V. Il'ina,¹ N.N. Rudyk,¹ O.I. Soboleva,¹ M.R. Polyvianova,¹ S.A. Khubezhov,² O.I. Il'in¹

¹ Institute of Nanotechnologies, Electronics and Equipment Engineering, Southern Federal University, 347922 Taganrog, Russia

² Khetagurov North Ossetian State University, 362025 Vladikavkaz, Russia

e-mail: mailina@sfedu.ru, nnrudyk@sfedu.ru

Received April 18, 2023

Revised April 18, 2023

Accepted April 18, 2023

The regularities of the influence of the growth temperature on the geometrical parameters, the concentration of the dopant nitrogen and the type of defects formed in carbon nanotubes grown on a molybdenum sublayer are established in this paper. It is shown that the best piezoelectric and resistive properties are observed in nitrogen-doped carbon nanotubes (N-CNTs) grown at a temperature of 525°C, which is due to the highest concentration of dopant nitrogen and high aspect ratio of nanotubes. Based on the results of thermodynamic analysis, the dependence of the dopant nitrogen concentration and the defect type on the tendency to form molybdenum nitrides and carbides during the growth of N-CNTs is shown. The obtained results can be used in the development of nanopiezotronic devices based on arrays of vertically aligned N-CNTs: nanogenerators, strain sensors and memory elements.

Keywords: carbon nanotubes, PECVD, nanopiezotronics, nitrogen defects, piezoelectric response, X-ray photoelectron spectroscopy.

DOI: 10.61011/TP.2023.07.56630.94-23

Introduction

Recent studies show that nitrogen-doped carbon nanotubes (N-CNT) are promising materials for the development of devices for converting and storing electrical energy [1–4]. This is due to the fact that the introduction of nitrogen atoms into the CNT structure leads to a significant change in its electrical properties and an increase in the catalytic activity of N-CNT [5,6]. In addition, in 2018, it was experimentally established that N-CNTs can also exhibit anomalous piezoelectric properties [7,8], which opened up great prospects for their application in nanopiezotronics — the direction of electronics using the internal piezoelectric field of deformed nanostructures to control the process of foaming charge carriers in them in order to implementation of a new generation of energy-efficient memory elements, nanogenerators and sensor devices [9]. The main advantage of nanopiezotronics devices is the ability of piezoelectric nanostructures to efficiently convert the mechanical energy of the environment into electrical energy, which ensures the independence of their operation. Thus, it is expected that self powered sources based on piezoelectric nanogenerators can become an alternative to modern batteries that have a limited service life and have a negative impact on the environment due to the presence of lithium in their composition.

N-CNTs are one of the promising materials for the implementation of nanopiezotronics devices due to the

combination of unique mechanical, piezoelectric and chemical properties of [10]. At the same time, the vertical orientation of the nanotubes relative to the substrate is preferable for high sensitivity (the ratio of the generated electric potential to the external mechanical force) N-CNT to external mechanical influences. The method of plasma-enhanced chemical vapor deposition [11] is used for growing vertically aligned N-CNTs. At the same time, the geometric and structural parameters of vertically aligned N-CNTs are significantly influenced by the material of the sublayer acting as the lower electrode of nanopiezotronics devices based on them. So, earlier we showed that N-CNTs grown on a molybdenum sublayer [12] have the greatest piezoelectric response. This dependence was associated with a sufficiently high concentration of dopant nitrogen (about 12%) in N-CNTs, caused by slight nitrogen diffusion into the Mo sublayer during the growth of nanotubes [12]. On the contrary, active formation of the corresponding nitrides was observed on the Ti, TiN and Cr sublayers during the interaction of ammonia with the sublayer material, which reduced the concentration of free nitrogen capable of embedding into the crystal lattice of the nanotube [12]. In addition, we found that the piezoelectric strain coefficient of N-CNTs decreases with an increase in the growth temperature (from 615 to 690°C) due to a decrease in the concentration of defects [13]. However, the growth of N-CNTs on molybdenum at lower temperatures was not studied, and this study will address this.

The impact of the growth temperature (below 600°C) on the geometric parameters, concentration and types of nitrogen dopant introduction in vertically aligned N-CNTs grown on a molybdenum sublayer is theoretically and experimentally studied in this paper.

1. Methods and approaches

The experimental samples of vertically aligned N-CNTs grown using the method of plasma-enhanced chemical vapor deposition (PECVD) at a growth temperature from 475 to 600°C. The flow C_2H_2 was 70 cm³/min, the flow NH_3 was 210 cm³/min. The pressure in the reactor during the process was maintained at 4.5 Torr. *p*-Si(100) was used as a substrate, on the surface of which a Mo film with a thickness of 100 nm and a Ni film with a thickness of 10 nm were deposited by magnetron sputtering using AUTO 500 (BOC Edwards, UK). The geometric parameters of N-CNTs were studied by scanning electron microscopy (SEM) at the Nova Nanolab 600 facility (FEI, the Netherlands), and the chemical composition was determined by X-ray photoelectron spectroscopy (XPS) at the K-Alpha Thermo Scientific spectrometer (Thermo Fisher Scientific).

The piezoelectric and resistive properties of N-CNTs were studied by atomic-force microscopy in the mode of piezoelectric force microscopy and current spectroscopy, respectively. A commercial NSG10 probe with a TiN conductive coating was used as the upper electrode. The piezoelectric strain coefficient d_{33} was determined based on the slope angle tangent of the dependence of the nanotube deformation on the amplitude of the applied alternating voltage $U = U_{DC} + U_{AC}(\sin \varphi t)$ at $U_{DC} = \pm 10$ V and $U_{AC} = \pm 3$ V with a frequency of $\varphi = 5$ kHz. The current-voltage curve (CVC) of N-CNTs were measured by applying a sawtooth voltage pulse with an amplitude of ± 4 V. The ratio of N-CNT resistances in the high- and low-resistance states (HRS/LRS) was calculated at a reading voltage of 1 V. The pressing force the AFM probe to the top of the nanotube during the measurement of the CVC was about 2 μ N.

The thermodynamic parameters of chemical reactions occurring between the materials of the catalytic layer of nickel, the lower electrode and the silicon substrate (*p*-Si) during the PECVD were calculated using specialized software FactSage 6.2 (GTT Technologies, Germany). The parameters of chemical reactions were evaluated by analyzing phase diagrams and temperature dependences of the change in Gibbs free energy $\Delta G(T)$, determined by the difference in enthalpy $\Delta H(T)$ and the product of the change in entropy $\Delta S(T)$ and the process temperature T .

The calculations took into account the thickness of the films of the catalytic nickel layer (10 nm), the lower electrode (100 nm) and the substrate (380 μ m), as well as the possibility of oxidation of the catalytic nickel layer in the air atmosphere and the possibility of formation of compounds between the materials of the catalyst and the

lower electrode. The calculations also took into account stoichiometric coefficients of chemical reactions, which are not given in this paper for the convenience of information perception.

As is known, the process of growing N-CNTs using the method of PECVD consists of four stages: heating of the sample, activation of catalytic centers, growth of N-CNTs, cooling of the sample. At the heating stage, a mixture of argon (Ar) gases with a flow of 40 cm³/min and ammonia (NH_3) with a flow of 15 cm³/min is fed into the chamber of PECVD, while the pressure in the chamber is maintained at 4.5 Torr. At this stage, the fragmentation of the initial film structure of the catalytic layer occurs with the formation of catalytic centers (CC), whose geometric dimensions, density and chemical composition affect the parameters of the grown N-CNTs. At the activation stage, the formed CC are subjected to additional exposure in the ammonia stream (210 cm³/min) at a given temperature, resulting in partial or complete reduction of the CC metal. Carbonaceous gas C_2H_2 and nitrogen-containing gas NH_3 are fed into the reaction chamber at the growth stage. At this stage, an important task is to maintain the optimal concentration of free carbon atoms and nitrogen atoms on the surface of the CC, responsible for the degree of doping and the ratio of forming defects of carbon substitution with nitrogen between pyridine, graphite and pyrrole types [4].

2. Thermodynamic analysis

2.1. Reactions at the heating stage

Thermodynamic analysis has shown that an oxidation reaction with the formation of NiO is possible when the film of the catalytic nickel layer is located outside the chamber, as well as in the residual atmosphere of the chamber at the heating stage. In addition, taking into account the small thickness of the Ni (10 nm) film, it can be assumed that NiO is formed along the entire thickness of the catalytic layer, as a result of which oxidation of the lower electrode material is possible when interacting with NiO.

The analysis of reactions at the heating stage in the structure with Mo showed that both oxidation of molybdenum MoO_2 and its binding to the catalyst material to form $MoNi_3$ is possible. At the same time, the growth of MoO_2 and $MoNi_3$ films deep into the structure leads to the possibility of a chemical reaction with the Si substrate, resulting in the formation of molybdenum disilicide ($MoSi_2$). At the same time, it is impossible to exclude the blocking of oxygen access to the volume of the molybdenum film by the oxidized upper layer and a change in the composition of the film in depth.

2.2. Reactions at the activation stage

At the activation stages, the ammonia can be decomposed into hydrogen and nitrogen at temperatures above 40°C. The resulting hydrogen can interact with NiO, reducing it to

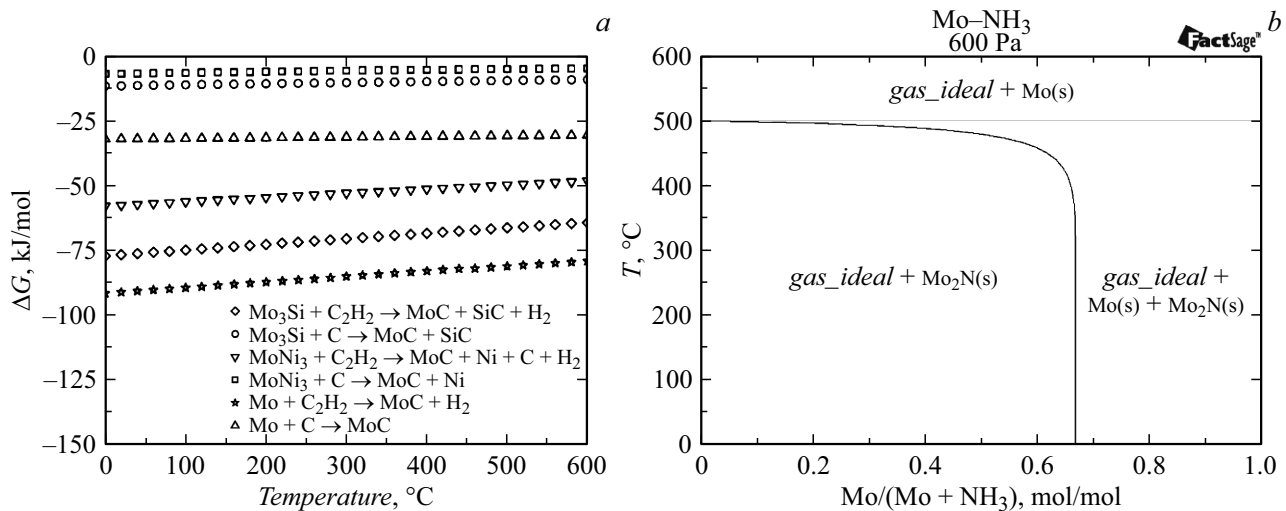
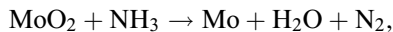


Figure 1. Temperature dependences of the Gibbs free energy change of the reactions of the interaction of the molybdenum sublayer with acetylene (a) and the phase diagram of the interaction of the molybdenum sublayer with ammonia (b).

metallic nickel with the formation of water vapor removed by the vacuum system. At the same time, nickel and molybdenum compounds formed at the heating stage do not interact with ammonia at the activation stage.

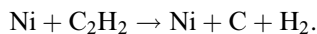
However, it is possible to recover molybdenum from MoO_2 and MoSi_2 both when interacting with ammonia and with hydrogen produced in case of dissociation of ammonia:



as a result, compounds with nickel MoNi_3 remain on the surface of the lower molybdenum electrode after the activation stage, and reduced molybdenum and its disilicide are present in the depth of the film.

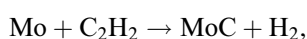
3. Reactions at the growth stage

Nickel does not react chemically with acetylene at the growth stage in the considered temperature range and at a given pressure, but leads to its thermal dissociation:



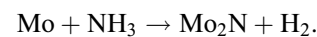
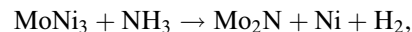
In this case, atomic carbon is produced, which, dissolving in the CC, leads to their supersaturation with carbon atoms, the release of carbon atoms to the surface of the CC and the formation of CNTs. Hydrogen atoms and molecules formed directly on the surface of the CC contribute to the removal of excess carbon atoms.

When acetylene interacts with a molybdenum sublayer, molybdenum carbide is formed (Fig. 1, a). The most likely reactions are



as a result of which part of the free carbon is drawn to the lower electrode to form molybdenum carbide, which leads to an increase in the ratio of free nitrogen and carbon and the predominant formation of pyrrole type nitrogen [4].

When ammonia interacts with a molybdenum sublayer at temperatures below 500°C , the following reactions are most likely to occur:



With an increase in temperature, the generation of molybdenum nitrides is not observed either for MoNi_3 or for Mo (Fig. 1, b).

Thus, a change in the growth temperature led to a redistribution of the ratio of free nitrogen and carbon necessary for the growth of N-CNTs, as a result of a change in the probability of the formation of molybdenum nitrides and carbides.

4. Results of experimental studies

Analysis of SEM images of arrays of vertically aligned N-CNTs showed that at 475°C , only the rudiments of N-CNT growth were formed, which is probably due to the insufficient rate of carbon diffusion to the growth center at low temperature (Fig. 2, a). The growth of vertically aligned N-CNTs was observed (Fig. 2, b–d) at growth temperatures over 500°C . The dependences of the diameter and length of grown N-CNTs on the growth temperature are shown in Fig. 3.

It is shown that the diameter of nanotubes increased on average from 55 ± 9 nm to 66 ± 23 nm with an increase in temperature from 500 to 600°C (Fig. 3, a), which is attributable to an increase of the rate of surface diffusion of nickel atoms and, as a consequence, an increase in the

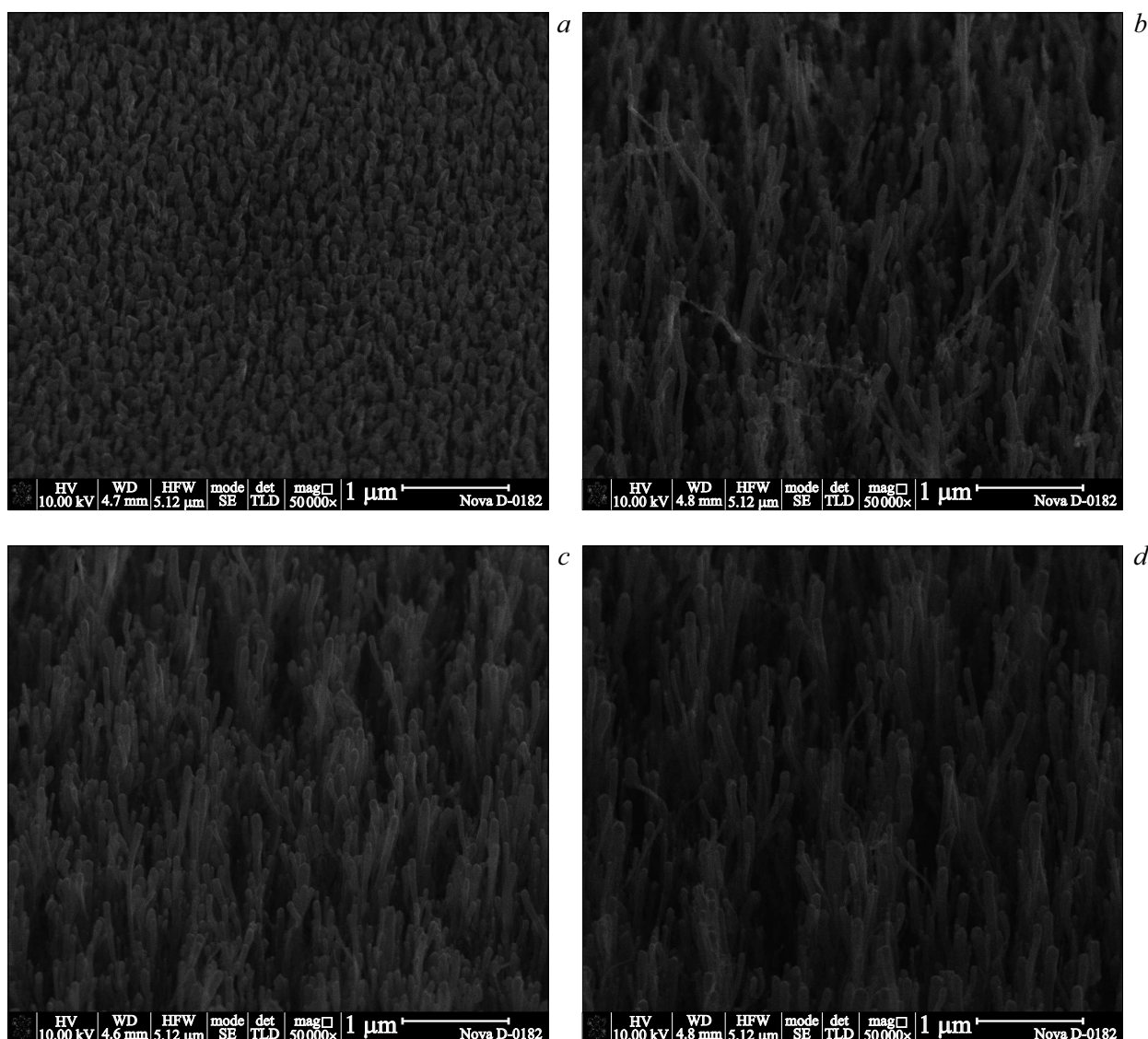


Figure 2. SEM images of N-CNTs obtained on a molybdenum sublayer and growth temperature: *a* — 475, *b* — 500, *c* — 550, *d* — 600°C.

diameter of the CC due to the merging of small catalytic centers. At the same time, the length of the N-CNT changed non-linearly with the increase of the temperature (Fig. 3, *b*), which may be attributable to changes in the concentration and types of defects of the dopant nitrogen [14].

The analysis of the XPS spectra showed that the maximum concentration of nitrogen (14 at.%) was observed in N-CNTs at a growth temperature of 525°C, then a decrease of the concentration of nitrogen dopant in N-CNTs to 11.2% (Fig. 4, *a*) was observed with an increase of the growth temperature. This dependence is attributable to the impact of two processes: a decrease in the probability of the formation of molybdenum nitride at a temperature above 500°C, leading to an increase in the concentration of free nitrogen, and a decrease in the probability of the formation of molybdenum carbide, leading to an increase in free carbon (Fig. 2).

The redistribution of the concentration ratio of free carbon and nitrogen atoms also led to the redistribution of nitrogen defects formed between pyridine, pyrrole and graphite types (Fig. 4, *b*). Thus, the maximum concentration of pyrrole-type nitrogen (30.8 at.%) and the minimum concentration of pyridine-type nitrogen (43.3 at.%) were observed at a temperature of 550°C. The concentration of pyrrole-type nitrogen decreased to 11 at.%, and the concentration of pyridine-type nitrogen increased to 66.1 at.% with a further increase of the temperature (Fig. 4, *b*). The concentration of pyrrole-type nitrogen was 23 at.%, the concentration of pyridine-type nitrogen was 54 at.% at a temperature of less than 550°C. This dependence is attributable, on the one hand, to the redistribution of the ratio of free carbon and nitrogen atoms, and on the other hand to the greater energy of the formation of pyridine-type nitrogen than pyrrole-type [15–17]. As a

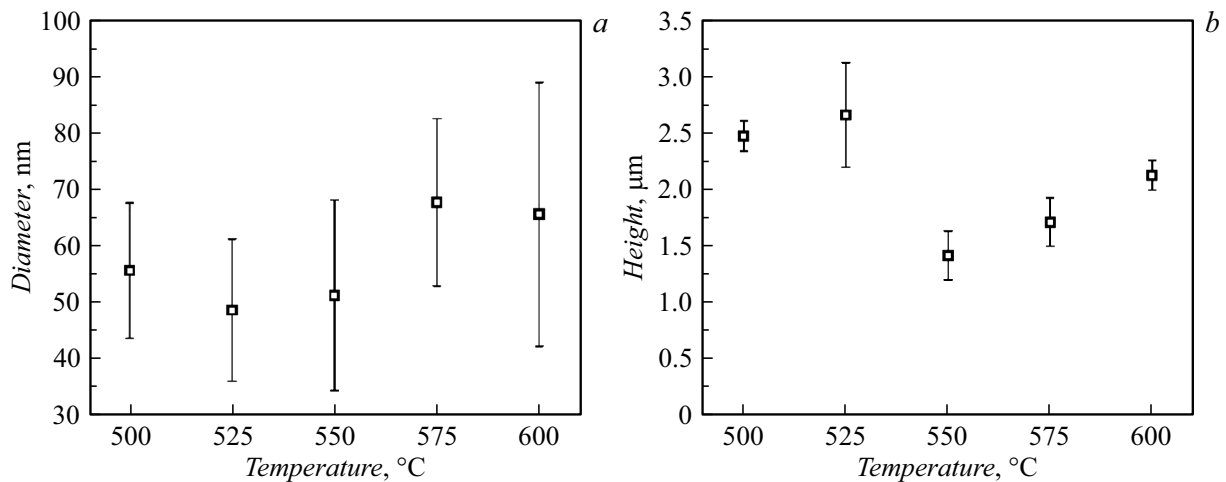


Figure 3. The impact of the growth temperature on the geometric parameters of the N-CNT: *a* — diameter, *b* — height.

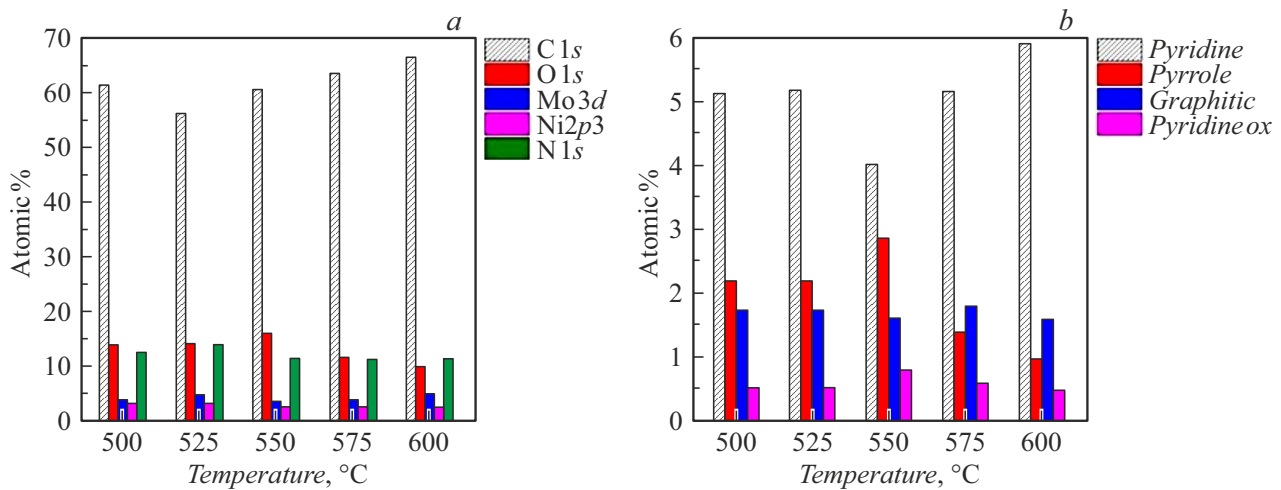


Figure 4. The impact of growth temperature on the chemical composition of N-CNTs: *a* — concentration of chemical elements, *b* — concentration of nitrogen defects of various types.

result, the concentration of pyrrole-type nitrogen sharply decreased with an increase of the growth temperature to 575°C and more. It should be noted that the change of the length of the N-CNT correlated with a change of the concentration of pyrrole-type nitrogen, which is consistent with the previously established dependence of the decrease of the length of the nanotube with an increase of pyrrole-type nitrogen [14].

A change of the dopant nitrogen and pyrrole-type nitrogen, in particular, with an increase in the growth temperature of N-CNTs, led to a nonlinear change of their piezoelectric and resistive properties (Fig. 5). Thus, the maximum values of the piezoelectric strain coefficient of N-CNTs d_{33} , quantitatively characterizing the deformation of the nanotube under the impact of external electric field and, conversely, the magnitude of polarization during deformation, and the resistance ratios in the high- and low-resistance states (HRS/LRS), were observed for N-CNTs

grown at 525°C (Fig. 5). The value of d_{33} was 23.8 pm/V, and the value of HRS/LRS was 22 at a reading voltage of 1 V. Then, the value of d_{33} decreased to 18.3 pm/V, and the value of HRS/LRS — to 4 with an increase of the growth temperature. The change of the piezoelectric and resistive properties of N-CNTs with an increase of the growth temperature correlates well with the change of the dopant nitrogen (Fig. 4, *a*). At the same time, a significant increase of d_{33} at a temperature of 525°C is probably due to the maximum ratio of the length of the nanotube to the diameter (about 57) [10]. An increase of d_{33} , in turn, led to an increase of the HRS/LRS ratio, since the reason for resistive switching in the N-CNT is the formation and subsequent redistribution of the piezoelectric potential formed during deformation of the nanotube [18]. The established pattern is consistent with the previously proposed mechanism of resistive switching in N-CNT [18,19] and can be used for the development of non-volatile memory elements.

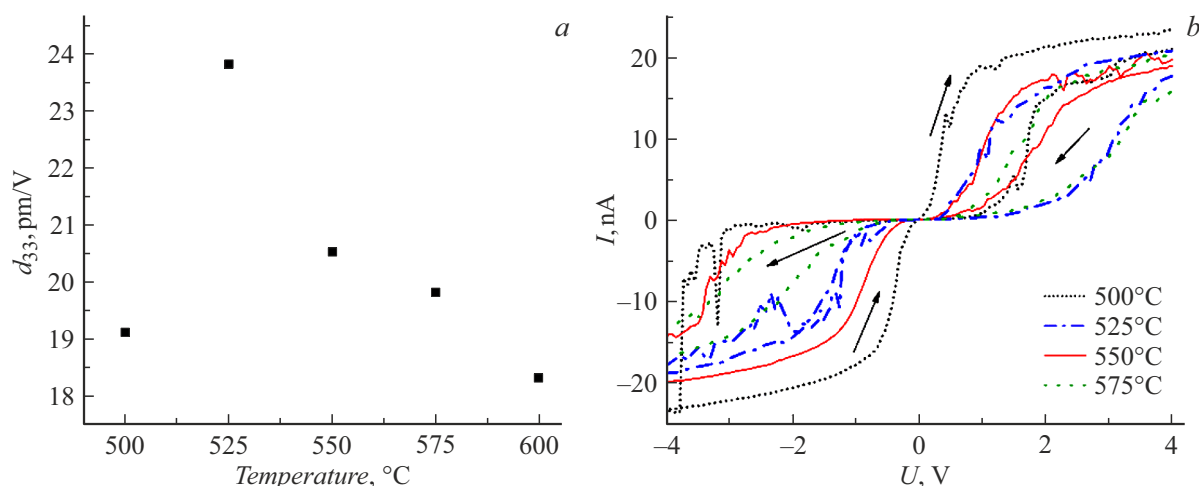


Figure 5. Experimental studies of N-CNTs grown at different temperatures: *a* — dependence of piezoelectric strain coefficient, *b* — dependence of resistive switching.

Conclusion

The regularities of the impact of the growth temperature on the geometric (diameter and height) and structural (concentration and types of defects of nitrogen dopant) parameters of N-CNTs grown on the lower Mo electrode are determined in the paper. Thermodynamic analysis of chemical reactions in the Ni/Mo/Si structure during the growing of N-CNTs by the method of plasma-enhanced chemical vapor deposition at the growth temperatures from 475 to 600°C was performed. It was shown that the best piezoelectric and resistive properties are observed in N-CNTs grown at a temperature of 525°C, which is attributable to the highest concentration of nitrogen dopant and the high aspect ratio of nanotubes. The results obtained can be used for the development of nanopiezotronics devices based on arrays of vertically aligned N-CNTs: nanogenerators, strain sensors and memory elements.

Funding

This study was supported by grant from the Russian Science Foundation № 22-79-10163, <https://rscf.ru/project/22-79-10163/> and was performed at the Southern Federal University. XPS measurements were performed using the equipment of the center for collective use „Physics and Technology of Nanostructures“ of North Ossetian State University after K.L. Khetagurov.

Conflict of interest

The authors declare that they have no conflict of interest.

References

- [1] S. Zhu, X. Dong, H. Huang, M.J. Qi. *Power Sources*, **459**, 228104 (2020). <https://doi.org/10.1016/j.powsour.2020.228104>
- [2] X. Li, J. Zhou, J. Zhang, M. Li, X. Bi, T. Liu, T. He, J. Cheng, F. Zhang, Y. Li, X. Mu, J. Lu, B. Wang. *Adv. Mater.*, **31** (39), 1 (2019). <https://doi.org/10.1002/adma.201903852>
- [3] W.Y. Shin, H.M. Jeong, B.G. Kim, J.K. Kang, J.W. Choi. *Nano Lett.*, **12** (5), 2283 (2012). <https://doi.org/10.1021/nl3000908>
- [4] M. Il'ina, O. Il'in, O. Osotova, S. Khubezhov, N. Rudyk, I. Pankov, A. Fedotov, O. Ageev. *Carbon N.Y.*, **190**, 348 (2022). <https://doi.org/10.1016/j.carbon.2022.01.014>
- [5] S.H. Lim, H.I. Elim, X.Y. Gao, A.T.S. Wee, W. Ji, J.Y. Lee, J. Lin. *Phys. Rev. B-Condens. Matter. Mater. Phys.*, **73** (4), 1 (2006). <https://doi.org/10.1103/PhysRevB73045402>
- [6] R. Sánchez-Salas, S. Kashina, R. Galindo, A.K. Cuentas-Gallegos, N. Rayón-López, M. Miranda-Hernández, R. Fuentes-Ramírez, F. López-Urías, E. Muñoz-Sandoval. *Carbon N.Y.*, **183**, 743 (2021). <https://doi.org/10.1016/j.carbon.2021.07.033>
- [7] M. Il'ina, O. Il'in, Y. Blinov, A. Konshin, B. Konoplev, O. Ageev. *Materials (Basel)*, **11** (4), 638 (2018). <https://doi.org/10.3390/ma11040638>
- [8] M.V. Il'ina, O.I. Il'in, A.V. Guryanov, O.I. Osotova, Y.F. Blinov, A.A. Fedotov, O.A. Ageev. *J. Mater. Chem. C*, **18**, 6014 (2021). <https://doi.org/10.1039/D1TC00356A>
- [9] Z.L. Wang. *Adv. Mater.*, **19** (6), 889 (2007). <https://doi.org/10.1002/adma.200602918>
- [10] M.V. Il'ina, O.I. Soboleva, S.A. Khubezov, V.A. Smirnov, O.I. Il'in. *J. Low Power Electron. Appl.*, **13** (1), 11 (2023). <https://doi.org/10.3390/jlpeal13010011>
- [11] H. Chen, A. Roy, J.B. Baek, L. Zhu, J. Qu, L. Dai. *Mater. Sci. Eng. Reports*, **70** (3–6), 63 (2019). <https://doi.org/10.1016/j.mser.2010.06.003>
- [12] M.V. Il'ina, O.I. Osotova, N.N. Rudyk, S.A. Khubezhov, I.V. Pankov, O.A. Ageev, O.I. Il'in. *Diam. Relat. Mater.*, **126**, 109069 (2022). <https://doi.org/10.1016/j.diamond.2022.109069>
- [13] M.V. Il'ina, O.I. Il'in, N.N. Rudyk, O.I. Osotova, A.A. Fedotov, O.A. Ageev. *Nanomaterials*, **11** (11), 2912 (2021). <https://doi.org/10.3390/nano11112912>
- [14] O.A. Louchev. *Phys. Status Solidi Appl. Res.*, **193** (3), 585 (2022). [https://doi.org/10.1002/1521-396X\(200210\)193:3<585::AID-PSSA585>3.0.CO;2-Y](https://doi.org/10.1002/1521-396X(200210)193:3<585::AID-PSSA585>3.0.CO;2-Y)

- [15] E.A. Arkhipova, A.S. Ivanov, N.E. Strokova, S.E. Chernyak, A.V. Shumyantsev, K.I. Maslakov, S.V. Savilov, V.V. Lunin. Carbon N.Y., **125**, 20 (2017).
<https://doi.org/10.1016/j.carbon.2017.09.013>
- [16] S. Kundu, W. Xia, W. Busser, M. Becker, D.A. Schmidt, M. Havenith, M. Muhler. Phys. Chem. Chem. Phys., **12** (17), 4351 (2010). <https://doi.org/10.1039/B923651A>
- [17] R. Arrigo, M. Hävecker, R. Schlögl, D.S. Su. Chem. Commun., **40**, 4891 (2008). <https://doi.org/10.1039/B812769G>
- [18] M.V. Il'ina, O.I. Il'in, O.I. Osotova, S.A. Khubezhov, O.A. Ageev. Nanobiotechnology Reports, **16** (6), 821 (2021).
<https://doi.org/10.1134/S2635167621060082>
- [19] M.V. Il'ina, O.I. Il'in, Y.F. Blinov, V.A. Smirnov, A.S. Kolomiitsev, A.A. Fedotov, B.G. Konoplev, O.A. Ageev. Carbon N.Y., **123**, 514 (2017). <https://doi.org/10.1016/j.carbon.2017.07.090>

Translated by A.Akhtyamov